EUROPEAN ORGANIZATION FOR NUCLEAR RESEARCH

CERN-EP/90-33

9 March 1990

SEARCH FOR HEAVY CHARGED SCALARS IN Z^0 DECAYS

DELPHI Collaboration

Abstract

Using a sample of Z^0's corresponding to about 12 000 events, we have searched for the production of charged scalars, primarily charged Higgs particles, decaying into $\bar{c}sc\bar{s}$, $\tau\nu + jets$, and $\tau\nu\tau\nu$. The average detection efficiency is 20%. No candidate was found in the leptonic modes. Masses in the range up to $30 - 36 GeV/c^2$ are excluded, extending the mass domain covered by previous e^+e^- machines.

P.Abreu[16], W.Adam[37], F.Adami[28], T.Adye[27], G.D.Alekseev[12], J.V.Allaby[7], P.Allen[36], S.Almehed[19], F.Alted[36], S.J.Alvsvaag[4], U.Amaldi[7], E.Anassontzis[3], W.D.Apel[13], B.Asman[32], C.Astor Ferreres[30], J.E.Augustin[15], A.Augustinus[7], P.Baillon[7], P.Bambade[15], F.Barao[16], G.Barbiellini[34], D.Yu.Bardin[12], A.Baroncelli[29], O.Barring[19], W.Bartl[37], M.J.Bates[25], B.V.Batyunia[12], M.Baubillier[18], K.H.Becks[39], C.J.Beeston[25], P.Beilliere[6], I.Belokopytov[31], P.Beltran[9], D.Benedic[8], J.M.Benlloch[36], M.Berggren[32], D.Bertrand[2], S.Biagi[17], F.Bianchi[33], J.H.Bibby[25], M.S.Bilenky[12], P.Billoir[18], J.Bjarne[19], D.Bloch[8], P.N.Bogolubov[12], D.Bollini[5], T.Bolognese[28], M.Bonapart[22], Y.E.Bonyushkin[12], P.S.L.Booth[17], M.Boratav[18], P.Borgeaud[28], H.Borner[25], G.Borisov[31], C.Bosio[29], O.Botner[35], B.Bouquet[15], M.Bozzo[10], S.Braibant[7], P.Branchini[29], K.D.Brand[39], R.A.Brenner[11], C.Bricman[2], R.C.A.Brown[7], N.Brummer[22], J.M.Brunet[6], L.Bugge[24], T.Buran[24], H.Burmeister[7], C.M.Buttar[25], J.A.M.A.Buytaert[2], M.Caccia[20], M.Calvi[20], A.J.Camacho Rozas[30], J.E.Campagne[7], A.Campion[17], T.Camporesi[7], V.Canale[29], F.Cao[2], L.Carroll[17], C.Caso[10], E.Castelli[34], M.V.Castillo Gimenez[36], A.Cattai[7], F.R.Cavallo[5], L.Cerrito[29], P.Charpentier[7], P.Checchia[26], G.A.Chelkov[12], L.Chevalier[28], C.Chiccoli[5], P.V.Chliapnikov[31], V.Chorowicz[18], R.Cirio[33], M.P.Clara[33], J.L.Contreras[36], R.Contri[10], G.Cosme[15], F.Couchot[15], H.B.Crawley[1], D.Crennell[27], M.Cresti[26], G.Crosetti[10], N.Crosland[25], M.Crozon[6], J.Cuevas Maestro[30], S.Czellar[11], S.Dagoret[15], E.Dahl-Jensen[21], B.D'Almagne[15], M.Dam[7], G.Damgaard[21], G.Darbo[10], E.Daubie[2], M.Davenport[7], P.David[18], A.De Angelis[34], M.De Beer[28], H.De Boeck[2], W.De Boer[13], C.De Clercq[2], M.D.M.De Fez Laso[36], N.De Groot[22], B.De Lotto[34], C.De La Vaissiere[18], C.Defoix[6], D.Delikaris[7], P.Delpierre[6], N.Demaria[33], L.Di Ciaccio[29], A.N.Diddens[22], H.Dijkstra[7], F.Djama[8], J.Dolbeau[6], K.Doroba[38], M.Dracos[8], J.Drees[39], M.Dris[23], W.Dulinski[8], R.Dzhelyadin[31], D.N.Edwards[17], L.O.Eek[35], P.A.M.Eerola[11], T.Ekelof[35], G.Ekspong[32], J.P.Engel[8], V.Falaleev[31], A.Fenyuk[31], M.Fernandez Alonso[30], A.Ferrer[36], S.Ferroni[10], T.A.Filippas[23], A.Firestone[1], H.Foeth[7], E.Fokitis[23], F.Fontanelli[10], H.Forsbach[39], B.Franek[27], K.E.Fransson[35], P.Frenkiel[6], D.C.Fries[13], R.Fruhwirth[37], F.Fulda-Quenzer[15], H.Fuerstenau[13], J.Fuster[7], J.M.Gago[16], G.Galeazzi[26], D.Gamba[33], U.Gasparini[26], P.Gavillet[7], S.Gawne[17], E.N.Gazis[23], P.Giacomelli[5], K.W.Glitza[39], R.Gokieli[18], V.M.Golovatyuk[12], A.Goobar[32], G.Gopal[27], M.Gorski[38], V.Gracco[10], A.Grant[7], F.Grard[2], E.Graziani[29], M.H.Gros[15], G.Grosdidier[15], B.Grossetete[18], S.Gumenyuk[31], J.Guy[27], F.Hahn[39], M.Hahn[13], S.Haider[7], Z.Hajduk[14], A.Hakansson[19], A.Hallgren[35], K.Hamacher[39], G.Hamel De Monchenault[28], J.F.Harris[25], B.Heck[7], I.Herbst[39], J.J.Hernandez[36], P.Herquet[2], H.Herr[7], E.Higon[36], H.J.Hilke[7], T.Hofmokl[38], R.Holmes[1], S.O.Holmgren[32], J.E.Hooper[21], M.Houlden[17], J.Hrubec[37], P.O.Hulth[32], K.Hultqvist[32], D.Husson[8], B.D.Hyams[7], P.Ioannou[3], P.S.Iversen[4], J.N.Jackson[17], P.Jalocha[14], G.Jarlskog[19], P.Jarry[28], B.Jean-Marie[15], E.K.Johansson[32], M.Jonker[7], L.Jonsson[19], P.Juillot[8], R.B.Kadyrov[12], G.Kalkanis[3], G.Kalmus[27], G.Kantardjian[7], F.Kapusta[18], P.Kapusta[14], S.Katsanevas[3], E.C.Katsoufis[23], R.Keranen[11], J.Kesteman[2], B.A.Khomenko[12], B.King[17], H.Klein[7], W.Klempt[7], A.Klovning[4], P.Kluit[2], J.H.Koehne[13], B.Koene[22], P.Kokkinias[9], M.Kopf[13], M.Koratzinos[7], K.Korcyl[14], A.V.Korytov[12], B.Korzen[7], C.Kourkoumelis[3], T.Kreuzberger[37], J.Krolikowski[38], U.Kruener-Marquis[39], W.Krupinski[14], W.Kucewicz[20], K.Kurvinen[11], M.I.Laakso[11], C.Lambropoulos[9], J.W.Lamsa[1], L.Lanceri[34], D.Langerveld[22], V.Lapin[31], J.P.Laugier[28], R.Lauhakangas[11], P.Laurikainen[11], G.Leder[37], F.Ledroit[6], J.Lemonne[2], G.Lenzen[39], V.Lepeltier[15], A.Letessier-Selvon[18], E.Lieb[39], E.Lillestol[7], E.Lillethun[4], J.Lindgren[11], I.Lippi[26], R.Llosa[36], B.Loerstad[19], M.Lokajicek[12], J.G.Loken[25], A.Lopez[15], M.A.Lopez Aguera[30], D.Loukas[9], J.J.Lozano[36], R.Lucock[27], B.Lund-Jensen[35], P.Lutz[6], L.Lyons[25], G.Maehlum[7], J.Maillard[6], A.Maltezos[9], S.Maltezos[23], F.Mandl[37], J.Marco[30], J.C.Marin[7], A.Markou[9], L.Mathis[6], C.Matteuzzi[20], G.Matthiae[29], M.Mazzucato[26], M.Mc Cubbin[17], R.Mc Kay[1], E.Menichetti[33], C.Meroni[20], W.T.Meyer[1], M.Michael[23], W.A.Mitaroff[37], G.V.Mitselmakher[12], U.Mjoernmark[19], T.Moa[32], R.Moeller[21], K.Moenig[39], M.R.Monge[10], P.Morettini[10], H.Mueller[13], H.Muller[7], G.Myatt[25], F.Naraghi[18], U.Nau-Korzen[39], F.L.Navarria[5], P.Negri[20], B.S.Nielsen[21], M.Nigro[26], V.Nikolaenko[31], V.Obraztsov[31], R.Orava[11], A.Ostankov[31], A.Ouraou[28], R.Pain[18], K.Pakonski[14], H.Palka[14], T.Papadopoulou[23], L.Pape[7], P.Pasini[5], A.Passeri[29], M.Pegoraro[26], V.Perevozchikov[31], M.Pernicka[37], M.Pimenta[16], O.Pingot[2], C.Pinori[26], A.Pinsent[25], M.E.Pol[16], G.Polok[14], P.Poropat[34], P.Privitera[5], A.Pullia[20], J.Pyyhtia[11], A.A.Rademakers[22], D.Radojicic[25], S.Ragazzi[20], W.H.Range[17], P.N.Ratoff[25], A.L.Read[24], N.G.Redaelli[20], M.Regler[37], D.Reid[17], P.B.Renton[25], L.K.Resvanis[3], F.Richard[15], J.Ridky[12], G.Rinaudo[33], A.Romero[33], P.Ronchese[26], E.Rosenberg[1], E.Rosso[7], P.Roudeau[15], T.Rovelli[5], V.Ruhlmann[28], A.Ruiz[30], H.Saarikko[11], D.Sacco[29], Y.Sacquin[28], E.Sanchez[36], E.Sanchis[36], M.Sannino[10], M.Schaeffer[8], H.Schneider[13], F.Scuri[34],

A.Sebastia[36], A.M.Segar[25], R.Sekulin[27], M.Sessa[34], G.Sette[10], R.Seufert[13], R.C.Shellard[7], P.Siegrist[28], P.Simone[33], S.Simonetti[10], F.Simonetto[26], A.N.Sissakian[12], T.B.Skaali[24], J.Skeens[1], G.Skjevling[24], G.Smadja[28], G.R.Smith[27], R.Sosnowski[38], K.Spang[21], T.Spassoff[12], E.Spiriti[29], S.Squarcia[10], H.Staeck[39], C.Stanescu[29], G.Stavropoulos[9], F.Stichelbaut[2], A.Stocchi[20], J.Strauss[37], R.Strub[8], C.Stubenrauch[7], M.Szczekowski[38], M.Szeptycka[38], P.Szymanski[38], S.Tavernier[2], E.Tchernyaev[31], G.Theodosiou[9], A.Tilquin[6], J.Timmermans[22], L.G.Tkatchev[12], D.Z.Toet[22], L.Tortora[29], D.Treille[7], U.Trevisan[10], G.Tristram[6], C.Troncon[20], E.N.Tsyganov[12], M.Turala[14], R.Turchetta[8], M.L.Turluer[28], T.Tuuva[11], I.A.Tyapkin[12], M.Tyndel[27], S.Tzamarias[7], F.Udo[22], S.Ueberschaer[39], V.A.Uvarov[31], G.Valenti[5], E.Vallazza[33], J.A.Valls[36], G.W.Van Apeldoorn[22], P.Van Dam[22], W.K.Van Doninck[2], N.Van Eijndhoven[7], C.Vander Velde[2], J.Varela[16], P.Vaz[16], G.Vegni[20], M.E.Veitch[25], E.Vela[36], J.Velasco[36], L.Ventura[26], W.Venus[27], F.Verbeure[2], L.Vibert[18], D.Vilanova[28], L.Viseu Melo[16], E.V.Vlasov[31], A.S.Vodopianov[12], M.Vollmer[39], G.Voulgaris[3], M.Voutilainen[11], V.Vrba[12], H.Wahlen[39], C.Walck[32], F.Waldner[34], M.Wayne[1], P.Weilhammer[7], J.Werner[39], A.M.Wetherell[7], J.H.Wickens[2], J.Wikne[24], W.S.C.Williams[25], M.Winter[8], G.Wormser[15], K.Woschnagg[35], N.Yamdagni[32], A.Zaitsev[31], A.Zalewska[14], P.Zalewski[38], E.Zevgolatakos[9], G.Zhang[39], N.I.Zimin[12], A.I.Zinchenko[12], R.Zitoun[18], R.Zukanovich Funchal[6], G.Zumerle[26], J.Zuniga[36]

(Submitted to Physics Letters B)

[1]Ames Laboratory and Department of Physics, Iowa State University, AMES IA 50011, U. S. A.
[2]Physics Department, Univ. Instelling Antwerpen, Universiteitsplein 1, B-2610 WILRIJK.
IIHE, ULB-VUB, Pleinlaan 2, B-1050 BRUXELLES.
Service de Phys. des Part. Elém., Faculté des Sciences, Université de l'Etat Mons, Av. Maistriau 19, B-7000 MONS.
[3]Physics Laboratory, University of Athens, Solonos Str. 104, GR-10680 ATHENS.
[4]Department of Physics, University of Bergen, Allégaten 55, N-5007 BERGEN.
[5]Dipartimento di Fisica, Università di Bologna and INFN, Via Irnerio 46, I-40126 BOLOGNA.
[6]Collège de France, Lab. de Physique Corpusculaire, 11 pl. M. Berthelot, F-75231 PARIS CEDEX 5.
[7]CERN, CH-1211 GENEVA 23.
[8]Division des Hautes Energies, CRN - Groupe DELPHI, B.P. 20 CRO, F-67037 STRASBOURG CEDEX.
[9]Greek Atomic Energy Commission, Nucl. Research Centre Demokritos, P.O. Box 60228, GR-15310 AGHIA PARASKEVI.
[10]Dipartimento di Fisica, Università di Genova and INFN, Via Dodecaneso 33, I-16146 GENOVA.
[11]Dept. of High Energy Physics, University of Helsinki, Siltavuorenpenger 20 C, SF-00170 HELSINKI 17.
[12]Joint Institute for Nuclear Research, Dubna, Head Post Office, P.O. Box 79, 101 000 MOSCOW, U.R.S.S.
[13]Institut für Experimentelle Kernphysik, Universität Karlsruhe, Postfach 6980, D-7500 KARLSRUHE 1.
[14]High Energy Physics Laboratory, Institute of Nuclear Physics, Ul. Kawiory 26 a, PL-30055 KRAKOW 30.
[15]Université de Paris-Sud, Lab. de l'Accélérateur Linéaire, Bat 200, F-91405 ORSAY.
[16]LIP, Av. Elias Garcia 14 - 1e, P-1000 LISBOA CODEX.
[17]Department of Physics, University of Liverpool, P.O. Box 147, GB - LIVERPOOL L69 3BX.
[18]LPNHE, Universités Paris VI et VII, Tour 33 (RdC), 4 place Jussieu, F-75230 PARIS CEDEX 05.
[19]Department of Physics, University of Lund, Sölvegatan 14, S-22363 LUND.
[20]Dipartimento di Fisica, Università di Milano and INFN, Via Celoria 16, I-20133 MILANO.
[21]Niels Bohr Institute, Blegdamsvej 17, DK-2100 COPENHAGUE 0.
[22]NIKHEF-H, Postbus 41882, NL-1009 DB AMSTERDAM.
[23]National Technical University, Physics Department, Zografou Campus, GR-15773 ATHENS.
[24]Physics Department, University of Oslo, Blindern, N-1000 OSLO 3.
[25]Nuclear Physics Laboratory, University of Oxford, Keble Road, GB - OXFORD OX1 3RH.
[26]Dipartimento di Fisica, Università di Padova and INFN, Via Marzolo 8, I-35131 PADOVA.
[27]Rutherford Appleton Laboratory, Chilton, GB - DIDCOT OX11 OQX.
[28]CEN-Saclay, DPhPE, F-91191 GIF-SUR-YVETTE CEDEX.
[29]Istituto Superiore di Sanità, Ist. Naz. di Fisica Nucl. (INFN), Viale Regina Elena 299, I-00161 ROMA.
Dipartimento di Fisica, Università di Roma II and INFN, Tor Vergata, I-00173 ROMA.
[30]Facultad de Ciencias, Universidad de Santander, av. de los Castros, E - 39005 SANTANDER.
[31]Inst. for High Energy Physics, P.O. Box 35, Protvino, SERPUKHOV (Moscow Region), U.R.S.S.
[32]Institute of Physics, University of Stockholm, Vanadisvägen 9, S-113 46 STOCKHOLM.
[33]Dipartimento di Fisica Sperimentale, Università di Torino and INFN, Via P. Giuria 1, I-10125 TORINO.
[34]Dipartimento di Fisica, Università di Trieste and INFN, Via A. Valerio 2, I-34127 TRIESTE.
Istituto di Fisica, Università di Udine, I-33100 UDINE.
[35]Department of Radiation Sciences, University of Uppsala, P.O. Box 535, S-751 21 UPPSALA.
[36]Inst. de Fisica Corpuscular IFIC, Centro Mixto Univ. de Valencia-CSIC, Avda. Dr. Moliner 50, E-46100 BURJASSOT (Valencia).
[37]Institut für Hochenergiephysik, Österreich Akad. d. Wissensch., Nikolsdorfergasse 18, A-1050 VIENNE.
[38]Inst. Nuclear Studies and, University of Warsaw, Ul. Hoza 69, PL-00681 WARSZAWA.
[39]Fachbereich Physik, University of Wuppertal, Postfach 100 127, D-5600 WUPPERTAL 1.

As often emphasized, e^+e^- machines offer a unique opportunity to search for heavy charged scalars, specifically Higgs particles, predicted by the most popular extensions of the standard model like supersymmetry and technicolor [1]. Previous searches have set limits against such particles up to 20 GeV/c^2 [2]. This paper extends these searches using a sample of 12 000 events collected with the DELPHI detector during the energy scan of the Z^0 performed at LEP at the end of 1989.

Charged Higgs particles and technicolor scalars have a precisely computable cross section which, given in terms of the neutrino cross section at the Z^0 reads [1] :

$$\sigma_{H^+H^-} = 1/2\cos^2 2\theta_w \beta_H^3 \sigma_{\nu\bar{\nu}} \approx 0.145\, \beta_H^3 \sigma_{\nu\bar{\nu}}$$

where

$$\beta_H = \sqrt{1 - \frac{4m_H^2}{m_{Z^0}^2}}$$

and where θ_W, the effective mixing angle appearing in Z^0 couplings, was taken from [3]. This cross section is relatively small and turns on rather slowly, due to a β_H^3 threshold factor which is characteristic of the p-wave production of a scalar. The angular distribution of the H^+ with respect to the e^+ incoming direction is proportional to $\sin^2\theta$.

A charged Higgs decays leptonically into $\tau\nu$ with a branching ratio BR ($H \rightarrow \tau\nu$) not fixed by the theory and we will use it as a free parameter. In one of the theoretically favoured models [1], the decay of heavy charged Higgs is dominated by $c\bar{s}$ and $\tau\nu$ final states with the ratio :

$$\frac{BR(H \rightarrow \tau\upsilon)}{BR(H \rightarrow c\bar{s})} \approx \frac{m_\tau^2 \tan^2\beta}{3(m_c^2 \cot^2\beta + m_s^2 \tan^2\beta)|V_{cs}|^2} \cong 0.5 \frac{\tan^4\beta}{1 + 10^{-2} \tan^4\beta}$$

where $\tan\beta = v_2/v_1$ is the ratio of vacuum expectations which appear in the two doublet model. The preferred values of $\tan\beta$ are larger than one, which means that BR ($H \rightarrow \tau\nu$) is greater than 1/3 and that it may even turn out that the $\tau\nu$ $\tau\nu$ final state becomes predominant . Nevertheless, our search covers also purely hadronic final states in $\bar{c}sc\bar{s}$ mode.

1. APPARATUS

A detailed description of the DELPHI detector, of the triggering conditions and of the analysis chain can be found in [4]. Here, only the specific properties relevant to the following analysis are summarized.

The charged tracks are measured in the 1.2 Tesla magnetic field by a set of three cylindrical tracking detectors: the Inner Detector (ID) covers radii 12 to 28 cm, the Time Projection Chamber (TPC) from 30 to 122 cm, and the Outer Detector (OD) between 197 and 208 cm. The end caps are covered by the Forward Chambers A and B, at polar angles

10^o to 36^o on each side. A layer of Time–of–Flight (TOF) counters is installed beyond the magnet coil for triggering purposes.

The electromagnetic energy is measured in the High Density Projection Chamber (HPC), and by the Forward Electromagnetic Calorimeter (FEMC) in the end caps. The HPC is a high granularity gaseous calorimeter covering polar angles 40^o to 140^o. For fast triggering a scintillation layer is installed after the first 5 radiation lengths of lead. The FEMC consists of 2×4500 lead glass blocks (granularity 1×1 degrees), covering polar angles from 10^o to 36^o on each side.

The trigger is based on the ID and OD coincidences, on the HPC and TOF scintillation counters, and on the forward detectors. The chamber trigger is formed using opposite quadrants of the OD in coincidence with the ID trigger layer. The counter trigger uses half length quadrants of TOF counters sensitive to penetrating particles, and HPC counters sensitive to electromagnetic showers with an energy > 2 GeV, arranged in various sets of back–to–back and majority logics. The forward trigger is made from the same side Chambers A and B coincidences, combined with the two FEMC signals in a majority logic. The efficiency of these various triggers is measured with the Z^0 data, by analyzing the recorded trigger patterns event–by–event.

The present analysis relies primarily on charged tracks reconstructed using the TPC, complemented by the Inner and the Outer detectors. This system reconstructs 98% of the charged tracks down to angles of 30^o. In some small azimuthal regions which correspond to six boundaries of the TPC sectors, this efficiency drops for energetic ($p > 4$ GeV/c) tracks. The electromagnetic calorimetry is used to veto against final state radiation in the $\tau\nu$ $\tau\nu$ analysis.

2. FOUR JET FINAL STATES

The search for $H^+H^- \rightarrow c\bar{s}\bar{c}s$ was performed by analyzing four jet hadronic final states. The jet–jet mass resolution is similar for the $c\bar{b}$ and $c\bar{s}$ systems within the investigated mass range. The four jet rate is however larger in case of $c\bar{b}$ decays, and therefore, the mass limits quoted in the following for the $c\bar{s}$ decay mode are also valid for the $c\bar{b}$ mode. The pairing method and the scaling of the jet–jet masses are based on the assumption of pair production of a heavy particle whose decay products are confined in separated hemispheres. Therefore, our search is limited to masses below 35 GeV/c^2.

The selected data consist of 5289 hadronic events having:

- at least 4 charged tracks with $p \geq 0.1$ GeV/c, and impact parameters $\delta_r \leq 4.0$ cm, $\delta_z \leq 10.0$ cm,
- total charged energy at least 15 GeV,

- $|\cos\theta_{thrust}| \leq 0.6$.

The jets were reconstructed using the Lund cluster algorithm for charged tracks with the default parameters [5]. The measured global jet variables have been compared with the Lund parton shower Monte Carlo predictions [6] and seen to be in good agreement with the simulation. The number of events classified as four jet events was 508, whereas we would expect 533 ± 16 events from the simulation.

For selecting events consistent with $e^+e^- \rightarrow H^+H^- \rightarrow 4$ jets we first selected 4 jet events and imposed general selections on the event topology, followed by mass dependent cuts optimized for three different Higgs masses in the search range.

In order to reject ambiguous multijet events due to soft gluon emission we required the smallest jet energy be at least 5 GeV and the total charged energy at least 40 GeV. The 4 jets were combined by choosing the pair (ij) with minimum opening angle. We corrected for missing neutrals by scaling the invariant jet–jet masses by the beam energy:

$$M_{ij}^{corrected} = E_{beam} * M_{ij} / (E_i + E_j)$$

To ensure that the scaling is justified and the missing momentum is equally shared between the jets, we demanded that the acollinearity between the momentum sum vectors of the two pairs is less than 25 degrees. Both scaling factors were required to be between 0.8 and 2.4. After these selections on the event topology we are left with 195 events. From the Lund parton shower Monte Carlo we retain 222 ± 10 events after the same cuts. Figs 1(a) and (b) represent the minimum opening angle between two jets and the difference between the scaled jet–jet masses after the general selections but before the mass dependent cuts. The data are shown with points and the solid line is obtained from the Lund parton shower Monte Carlo simulation. We conclude that the variables sensitive to the final selections are well reproduced by our simulation.

To exclude the background due to standard hadronic processes, we use mass dependent selections optimized to the Higgs pair production with a mass of 20, 25 and 30 GeV/c^2. The average minimum (maximum) jet–jet opening angle $\min\phi_{ij}$ ($\max\phi_{kl}$) grows about linearly from 45 (57) degrees up to 69 (93) degrees for this mass range, and the difference between the scaled jet–jet masses $\max M_{ij}^{corrected} - M_{kl}^{corrected}$ increases from 2.5 GeV/c^2 to 7.1 GeV/c^2. The selections and their efficiencies are shown in table 1, named as low, medium and high. The efficiencies, depicted also in fig. 1(c) were obtained by simulating Higgs pair production into 4 quark final states, which were fragmented with the Lund parton shower model.

TABLE 1 - Selections for charged Higgs hadronic final states

	Low mass	Medium mass	High mass
$\min\phi_{ij}$	$\geq 40^o$	$\geq 50^o$	$\geq 60^o$
$\max\phi_{kl}$	$\leq 60^o$	$\leq 90^o$	$\leq 100^o$
$\max\phi_{kl} - \min\phi_{ij}$	$\leq 13^o$	$\leq 15^o$	$\leq 17^o$
$\max M_{ij}^{corrected} - \min M_{kl}^{corrected}$	≤ 3.5 GeV/c^2	≤ 5.0 GeV/c^2	≤ 6.5 GeV/c^2
Efficiency	$(13 \pm 2)\%$	$(17 \pm 3)\%$	$(15 \pm 3)\%$

After imposing the final cuts, 8, 9 and 7 events remain after, respectively, the low, medium and high mass selections. The expected numbers of background events, averaged over the Lund parton shower and Marchesini–Webber [7] Monte Carlo simulations, are 5.6 ± 1.4 (stat.) ± 0.9 (syst.), 15.0 ± 2.6 (stat.) ± 1.9 (syst.) and 8.4 ± 2.0 (stat.) ± 1.9 (syst.). The systematic errors were estimated from the difference between the two models. In order to include them in our background estimate, we subtract one standard deviation from the expected numbers of events which are taken as 3.9, 11.8 and 5.6, respectively. After the same selections, the signal events would be 12.4 for a 20 GeV/c^2 Higgs, 13.0 for a 25 GeV/c^2 Higgs and 8.4 for a 30 GeV/c^2 Higgs, assuming the hadronic branching fraction equal to one.

By using Poisson statistics with the non–zero expected background, we obtain an excluded region between 18 and 31 GeV/c^2 for the Higgs pair production when $Br(H^+ \rightarrow c\bar{s}) = 1$ at 95% CL. The same region is excluded for the Higgs decay mode $c\bar{b}$. The full excluded region from the analysis of hadronic final states is shown in fig. 3 (curve a) as a function of the hadronic branching fraction.

3. $\tau\nu$ + JETS CHANNEL

For an intermediate Higgs mass, from 10 to 30 GeV/c^2, the decay products of H^+ and H^- can be well separated using the two hemispheres defined by the plane perpendicular to the thrust axis of the event. Since τ decays predominantly (86%) into one charged particle, we require a single charged particle of momentum above 3 GeV/c isolated in one hemisphere and, to get rid of the $\tau^+\tau^-$ background, more than four charged particles with a mass greater than 2.0 GeV/c^2 in the opposite hemisphere. To avoid smearing effects due to losses of charged particles in the forward region of the detector, we request a thrust axis of the event at more than 37^o from the beam axis, keeping a sample of 5955 hadronic Z^0's. As before, event reconstruction is based on charged tracks which have a distance of closest approach transverse to the beam axis of less than 4 cm and a longitudinal distance to the interaction point of less than 10 cm. But tracks with a transverse distance between 4 and

10 cm, which come primarily from decays and photon conversion, are taken into account to define the isolation criterion.

We define δ as the angle between the track isolated in one hemisphere and the thrust axis of the particles in the opposite hemisphere. In fig. 2(a) the distribution in δ shows a clear separation between the expected signal and the background. The data are compared to the background generated using the Lund 6.3 parton shower model [5] (referred to, for simplicity, as QCD in the rest of the text), and to the expected signal, assuming a charged Higgs mass of 20 GeV/c^2, and BR ($H \rightarrow \tau\nu$) = 0.3. The isolated particle coming from τ's is energetic and, provided that the Higgs mass is above 10 GeV/c^2, is emitted at angle with respect to the thrust axis of the opposite hemisphere. By asking for an angle greater than 20° and a momentum greater than 3 GeV/c, one removes all the background keeping an efficiency of $22 \pm 1.3\%$ for a 20 GeV/c^2 Higgs mass. In the real data, no event passes these cuts.

While the observed distribution shown in fig. 2(a) agrees in shape with the Monte Carlo distribution, the number of events is in slight excess, i.e. a 1.6 standard deviations effect, with respect to the expectation. To understand the origin of this disagreement, we notice that the isolation method critically depends on the distribution of low momentum tracks accompanying a single energetic track in the mechanism of jet fragmentation. We can measure this effect by relaxing the isolation criterion to allow for the presence of slow tracks with momentum smaller than 1 GeV/c. We observe 186 events with an average multiplicity $m = 3.15 \pm 0.15$ while the QCD Monte Carlo predicts 118 events with $m = 2.90 \pm 0.10$. Thus the observed discrepancy is also present in this larger subset, which represents 2% of the Z^0 hadronic decays, indicating an origin of the excess of events observed at low δ that is not related to Higgs production. This effect has however no practical implications for the heavy charged Higgs search since, as previously stated, no event remains after cuts.

For charged Higgs particles heavier than 30 GeV/c^2, this method does not apply since the jet opening angle is so large that the hemispheric separation becomes very inefficient. We thus select 3–jet events with one jet formed by only one particle with momentum above 5 GeV/c. Jets are reconstructed using the Lund cluster algorithm [5] with default parameters. Candidates excluded by the first method which, from fig. 2(a), appear heavily contaminated by QCD background, are not considered in the following. At this level we are left with 25 candidates while the Monte Carlo predicts 26 ± 3 events. One reaches a full separation from background by using other features which are manifest in this mass region : low thrust of the event, below 0.9, an acollinearity angle between the two jets greater than 50° and below 140°, in contrast to QCD jets which tend to be aligned. After performing these cuts which keep 18 ± 1.3 % of the $c\bar{s}\tau\nu$ decays at m_H = 35 GeV/c^2, one is left with no candidate while the Monte Carlo predicts a background of 0.5 ± 0.2 candidates.

Fig. 2(b) shows the variation of the efficiency of each method with the Higgs mass, assuming a $\tau\nu\ c\bar{s}$ channel. The two methods are combined to reach an almost constant efficiency without any contamination.

4. $\tau\nu\ \tau\nu$ CHANNEL

This channel has been searched for using acoplanar two particle final states. Since a major contamination is expected from final state radiation in lepton pair production, the analysis is restricted to a sample corresponding to 5500 hadronic Z^0 for which the electromagnetic calorimeters were fully operational.

For $m_H \leq 25$ GeV/c^2, the acceptance of the chamber trigger on two charged tracks, which imposes a loose back–to–back topology, is above 50%. For higher masses, we rely mostly on the electromagnetic trigger, and we require two showers of more than 3 GeV in the HPC or one shower in coincidence with the TOF counters. Since more than half of the τ decays provide electromagnetic energy, the global trigger efficiency for two–prong events is $(55 \pm 5)\%$. To check this figure, we have used $Z \rightarrow \tau\tau$ events triggered by the chamber trigger and measured the fraction which fulfils the electromagnetic trigger. From the agreement with the Monte Carlo prediction, we conclude that the simulation of the trigger is adequate and has a systematic uncertainty of the order of 10%.

After demanding two charged particles with a momentum larger than 2 GeV/c, with a polar angle between 30° and 150° and with an acoplanarity angle larger than 15°, one is left with $20 \pm 2\%$ of the $\tau\nu\ \tau\nu$ decays at $m_H = 30$ GeV/c^2. These selections eliminate the background coming from $\gamma\gamma \rightarrow l^+l^-$ and from $Z^0 \rightarrow \tau^+\tau^-$. The remaining 2 candidates in the data sample show an energetic isolated photon coplanar with the two charged tracks and at more than 30° from each of them, while a Monte Carlo generating lepton pairs with final state radiation [8] predicts 4 ± 0.5 events. We conclude that no candidate is left corresponding to the $\tau\nu\ \tau\nu$ topology.

5. RESULTS

Fig. 3 summarizes the limits, at 95% CL, obtained from the channels previously discussed. The excluded area largely extends the one covered at lower energies. For BR $(H \rightarrow \tau\nu) > 0.3$, masses up to 34–36 GeV/c^2 are excluded. This corresponds, as discussed in the introduction, to $tg\beta > 1$, a region favoured in theoretical models. Charged pseudoscalars $P^{\pm}$, which appear in technicolor theories and which would be produced with the same cross section, are also excluded, as long as their decay is dominated by the same channels.

In conclusion, Z^0 data provide an efficient and clean way to search for H^+H^- and, from a limited sample of data, the limits from lower energy machines have been significantly improved by using very distinct topologies.

Acknowledgements

We are greatly indebted to our technical staffs and collaborators and funding agencies for their support in building the DELPHI detector and to the many members of LEP Division for the speedy commissioning and superb performance of the LEP machine.

REFERENCES

[1] For recent reviews see, for instance:
S. Dawson et al., The Higgs Hunters's Guide to be published (1989);
P.J. Franzini et al., Z° Physics at LEP1, Higgs Search, CERN 89-08, Vol. 2, p. 59.

[2] W. Bartel et al., Zeitschr. für Phys. C31 (1986) 359;
H.-J. Behrend et al., Phys. Lett. B193 (1987) 376.

[3] See, for instance, G. Altarelli, Rapporteur's Talk at the XIV International Symposium on Lepton and Photon interactions, Stanford, CERN-TH 5562/89 (August 1989).

[4] P. Aarnio et al., Phys. Lett. B231 (1989) 539;
The DELPHI Detector (to be published).

[5] T. Sjöstrand, Comp. Phys. Comm. 27 (1982) 243, ibid. 28 (1983) 229;
T. Sjöstrand and M. Bengtsson, Comp. Phys. Comm. 43 (1987) 367.

[6] P. Aarnio et al., CERN/EP 90–19 (March 1990).

[7] G. Marchesini and B.R. Webber, Nucl. Phys. B238 (1984) 1.

[8] For $\mu^+\mu^-$ and e^+e^- channels, MUSTRAAL is used and KORALZ for $\tau^+\tau^-$:
See for instance, R. Kleiss, Z° Physics at LEP1, Event generators and software, CERN 89–08, Vol 3, p.69.

FIGURE CAPTIONS

FIGURE 1 4–jet analysis:

(a) Minimum opening angle between two jets after general selections on the 4–jet topology. Data points are shown together with the Lund parton shower simulation (solid line).

(b) Difference between the scaled jet–jet masses after the same selections as fig. 1(a).

(c) Detection efficiency as a function of charged Higgs mass. The three curves depict the efficiency in each mass range.

FIGURE 2 $\tau\nu$ + jet analysis:

(a) δ is the angle between the track isolated in one hemisphere and the thrust of the particles of the opposite hemisphere. The data are compared with (1) the background generated using the Lund 6.3 parton shower model and with (2) the charged Higgs production at a mass of 20 GeV/c^2, assuming BR ($H \rightarrow \tau\nu$) = 0.3. All distributions are normalized to the total number of events in the data.

(b) Dashed curve: efficiency of the hemispheric isolation method ($p > 3$ GeV/c, $\delta > 20^o$) versus the charged Higgs mass. Dashed dotted curve: efficiency to reconstruct an isolated track at $p > 5$ GeV/c with two additional jets forming an angle between 50^o and 140^o. Solid curve: efficiency of the combination of the two methods.

FIGURE 3 Excluded contours, at 95% CL, for $Z \rightarrow H^+H^-$, in terms of the hadronic branching ratio and of the charged Higgs mass.

Curve **a** corresponds to the 4 jet channel.

Curve **b** corresponds to the $\tau\nu\ c\bar{s}$ channel.

Curve **c** corresponds to the $\tau\nu\ \tau\nu$ channel.

Curve **b+c** combines these two channels in the overlapping regions.

The hatched area is obtained from PETRA results [2].

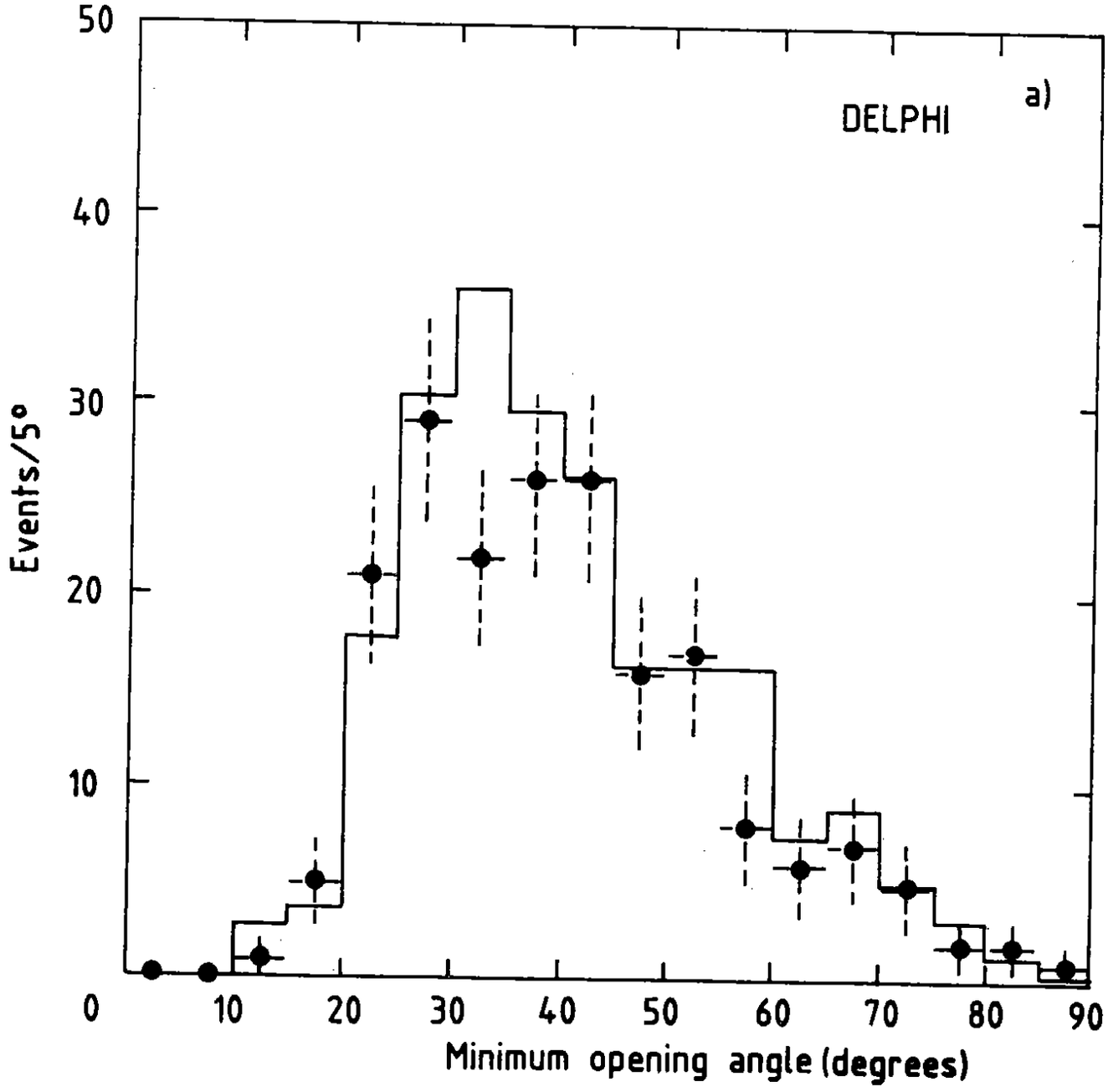
DELPHI
a)
Events/5°
Minimum opening angle (degrees)
0
10
20
30
40
50
60
70
80
90

Fig. 1 a)

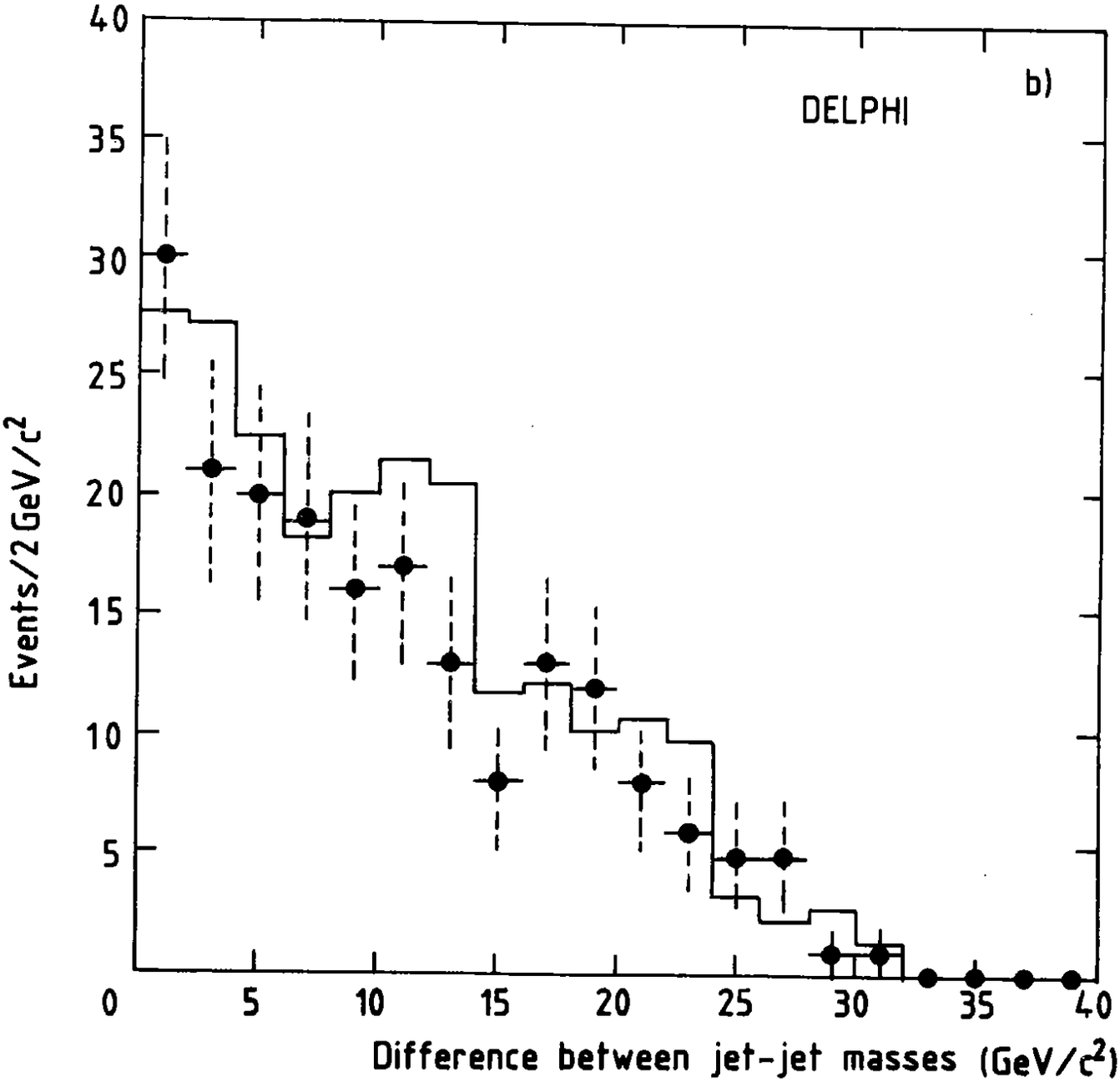
DELPHI
b)
Events/2 GeV/c²
Difference between jet-jet masses (GeV/c²)
0
5
10
15
20
25
30
35
40

Fig. 1 b)

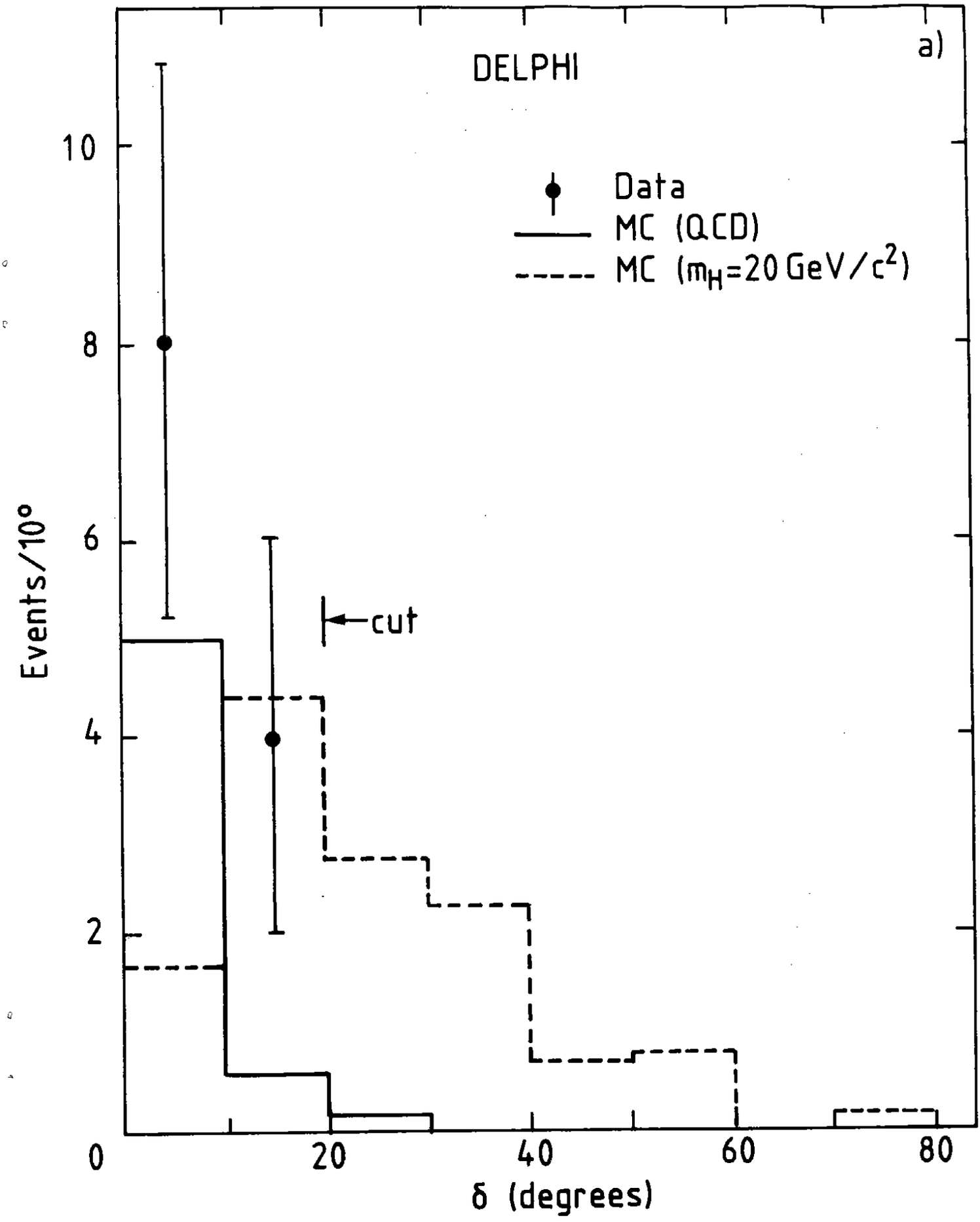
a)
DELPHI
Data
MC (QCD)
MC (m_H=20 GeV/c^2)
cut
Events/10°
δ (degrees)
0
2
4
6
8
10
20
40
60
80

Fig. 2 a)

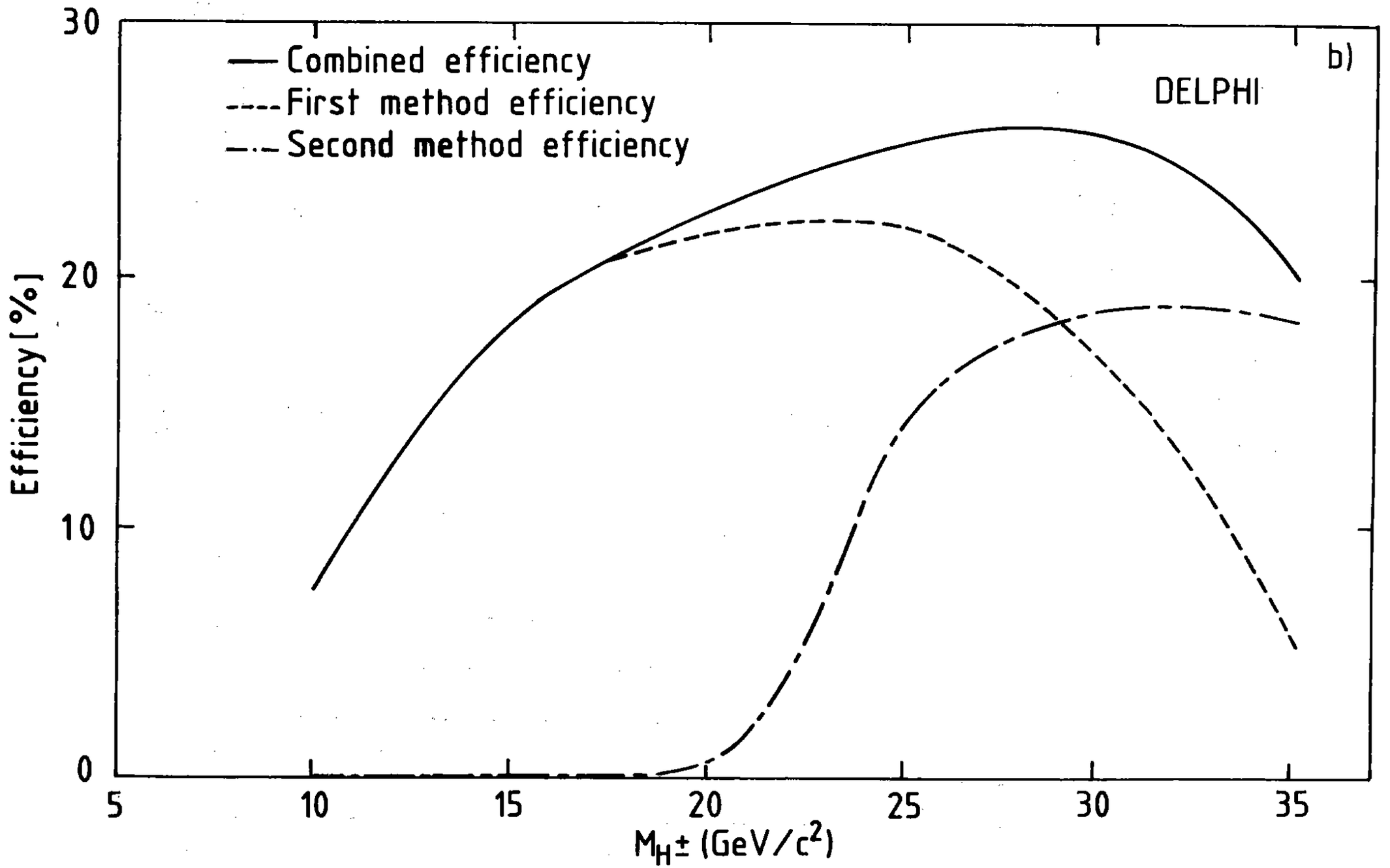
30
20
10
0
5
10
15
20
25
30
35
Efficiency [%]
$M_{H^\pm}$ (GeV/c^2)
Combined efficiency
First method efficiency
Second method efficiency
DELPHI
b)

Fig. 2 b)

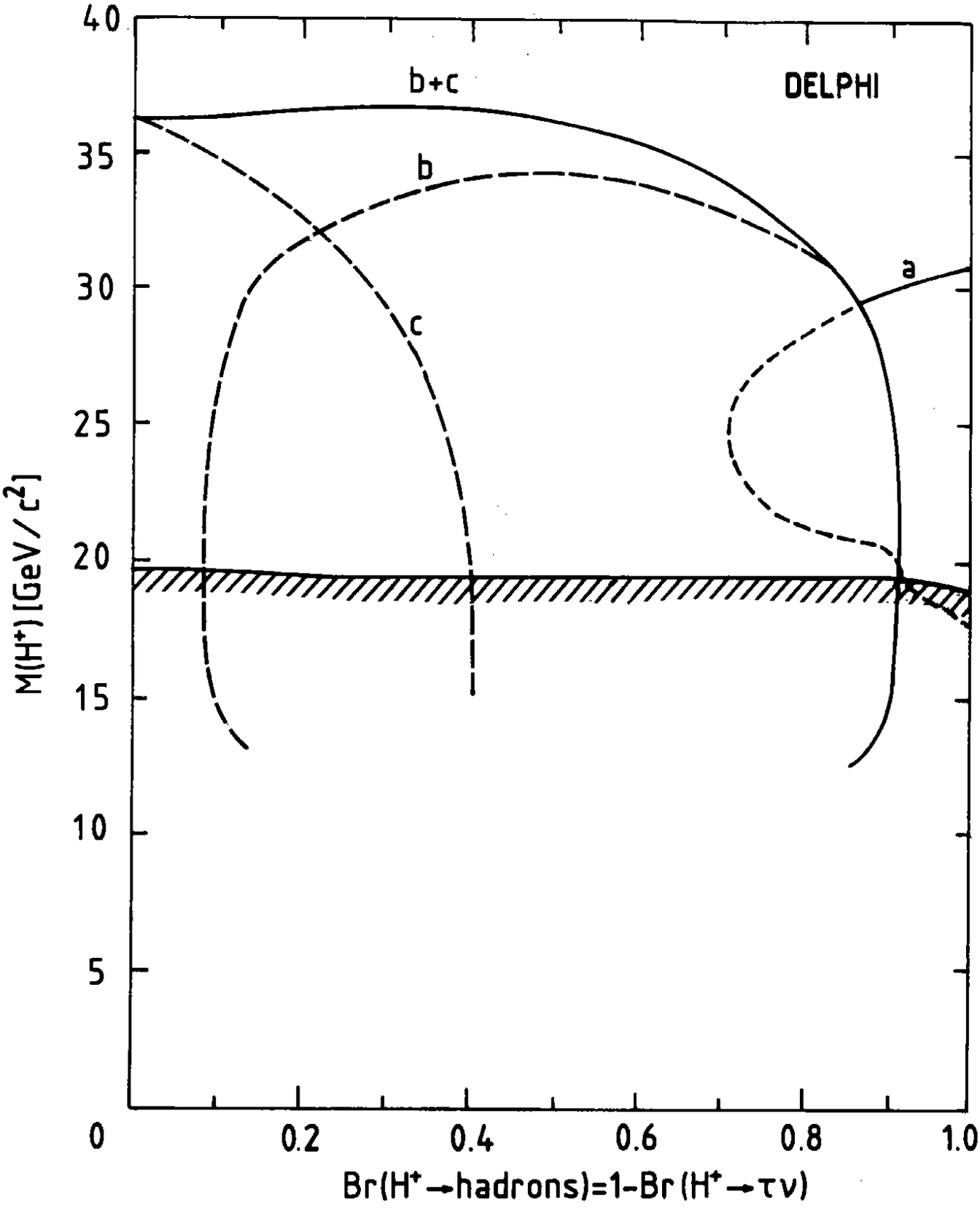
DELPHI
b+c
b
c
a
M(H⁺) [GeV/c²]
Br(H⁺→hadrons)=1-Br(H⁺→τν)
0
5
10
15
20
25
30
35
40
0.2
0.4
0.6
0.8
1.0

Fig. 3